

The spatial string tension and its effects on screening correlators in a thermal QCD plasma

Dibyendu Bala,¹ Olaf Kaczmarek,¹ Peter Petreczky,²

Sayantana Sharma,³ and Swagatam Tah^{3,*}

¹*Fakultät für Physik, Universität Bielefeld, D-33615 Bielefeld, Germany*

²*Physics Department, Brookhaven National Laboratory, Upton, New York 11973, USA*

³*The Institute of Mathematical Sciences,
a CI of Homi Bhabha National Institute, Chennai, 600113, India*

Abstract

We calculate the spatial Wilson line correlator for 2 + 1 flavor QCD using highly improved staggered quark discretization for fermions and in quenched QCD for a wide range of temperatures, from the chiral crossover temperature $T_{pc} \simeq 156$ MeV or the deconfinement temperature $\simeq 300$ MeV respectively, up to 2 GeV. Extracting the spatial string tension for different lattice cut-offs and by performing a continuum extrapolation of this observable, we show that the soft (magnetic) gluons interact non-perturbatively even at temperatures $\gtrsim 1$ GeV. We provide incriminating evidences to demonstrate that dimensionally reduced effective theories can describe these soft quark and gluon quasi-particles for both quenched and 2 + 1 flavor QCD, at temperatures $T \gtrsim 5T_{pc}$. We also show for the first time the imprints of the non-perturbative pseudo-potential in the properties of mesonic screening masses for temperatures ranging from 0.8-164 GeV in the quark-gluon plasma.

PACS numbers: 12.38.Gc, 11.15.Ha, 11.30.Rd, 11.15.Kc

* Corresponding author: swagatamt@imsc.res.in

Introduction: Quantum Chromodynamics (QCD) has a rich set of non-perturbative properties at finite temperatures [1, 2]. There is a transition from a phase of color-singlet degrees of freedom to a phase where color charges are deconfined when the temperature is increased, which occur through a first order phase transition [3] or a smooth crossover [4] respectively in QCD without and in the presence of dynamical quarks. Ab-initio lattice field theory calculations have demonstrated this and also determined the corresponding transition temperature which is $T_{dr0} = 0.7457(45)$ [5] for QCD without quarks (pure SU(3) gauge theory or quenched QCD), whereas it is $T_{pc} \simeq 156$ MeV [6–9] in presence of two degenerate light quarks and one strange quark flavor. In the deconfined phase of QCD with a gauge coupling g , two more scales apart from the temperature T are dynamically generated; the electric gT and the magnetic scale g^2T/π , which correspond to the inverse correlation lengths of the color-electric and color-magnetic degrees of freedom respectively. When these scales are well separated i.e. $g^2T/\pi \ll gT \ll \pi T$, the gauge and fermion fields with typical momenta $\sim \pi T$ can be integrated out [10] resulting in dimensionally reduced effective theory known as electro-static QCD (EQCD) [11, 12]. Within this effective field theory the temporal component of the gauge field A_0 appear as a static adjoint scalar field and the parameters of this theory i.e. the couplings g_E, λ_E and the Debye mass m_D can be calculated using perturbation theory to all orders in g [12, 13]. The high temperature phase in QCD correspond to the confined phase in a 3 dimensional adjoint Higgs theory [13, 14]. The confinement scale of this theory corresponds to the magnetic scale in QCD, which is inherently non-perturbative and gives rise to infrared divergences which cannot be tamed through perturbative resummations [15]. At higher temperatures, the A_0 fields become massive and can be integrated out from the QCD partition function, giving rise to an effective theory called magneto-static QCD (MQCD) which is a 3 dimensional pure gauge theory [12, 16, 17]. However it is not clear a priori at what temperatures such a clean separation of scales would occur to justify the validity of these effective theories to describe QCD [18, 19].

The non-perturbative magnetic sector in high temperature QCD can be directly accessed through the calculation of the spatial Wilson loop [20, 21]. Earlier lattice calculations have demonstrated the area-law behavior of the spatial Wilson loop, further extracting the spatial string tension σ_s from the linearly rising pseudo-potential at large distance scales in SU(3) without dynamical quarks [22–26] as well as in 2 + 1 flavor QCD with a heavier than

physical light quark mass [27]. An agreement with the estimate of σ_s in dimensional reduced theory was observed at $\gtrsim 2 T_{\text{pc}}$, and agreement between the EQCD calculations and lattice QCD data of different thermodynamic quantities like the quark number susceptibilities are typically observed at temperatures $\gtrsim 3 T_{\text{pc}}$ [28].

In this Letter, we revisit the calculation of the σ_s using sophisticated lattice QCD techniques to convincingly address the question *what temperature range* herald the onset of the dimensional reduction in QCD ? By performing a careful continuum extrapolation of the pseudo-potential extracted out of spatial Wilson line correlators calculated at two(three) different lattice cut-offs for a temperature range ~ 0.2 -1(2.7) GeV for QCD with(without) dynamical physical quarks, we demonstrate the onset of dimensional reduction at temperatures $\gtrsim 5 T_{\text{pc}}$ from a detailed understanding of its properties. We show for the first time that this non-perturbative potential describing the magnetic modes can remarkably explain the deviation of the screening masses of meson-like long-distance excitations at high temperatures 0.8-1.64 GeV from the perturbative EQCD prediction. We further quantify the spin-splitting between the vector and the pseudo-scalar screening excitations which cannot be addressed within the leading order perturbative EQCD framework [29].

Theoretical and numerical framework: In this work we extract the *confining* pseudo-potential and subsequently σ_s by measuring the correlation between two spatial Wilson lines $W(R, L)$ in modified-Coulomb gauge, each of which are of length L along the z direction separated by a transverse distance R in the x - y plane. We use spatial Wilson line correlators in modified-Coulomb gauge instead of the spatial Wilson loops because these have a much better signal to noise ratio and lead to the same pseudo-potential. This approach is often used to obtain the static potential in zero temperature QCD [30–34], and results in the same potential as the calculations using Wilson loops, see e.g. [35]. We implement the Wilson lines on a 4 dimensional Euclidean lattice with N sites along each spatial direction and N_τ sites along the temporal direction, τ and at each time-slice. We consider $N = 32, 40$ for 2+1 flavor QCD and $N = 32, 48, 64$ for pure $SU(3)$ with $N_\tau = N/4$ for each temperature $T = 1/(N_\tau \cdot a)$ which is varied between 0.16-1 GeV and 0.3-2.7 GeV respectively. The pseudo-potential $V(R)$ can be extracted from the ratio of expectation values of the spatial Wilson line correlators of length $z = L \cdot a$ and $z = (L + 1) \cdot a$ where $L \lesssim N$ from the relation,

$$V(R) \cdot a = \lim_{L \rightarrow \infty} \ln \left[\frac{\langle W(R, L) \rangle}{\langle W(R, L + 1) \rangle} \right]. \quad (1)$$

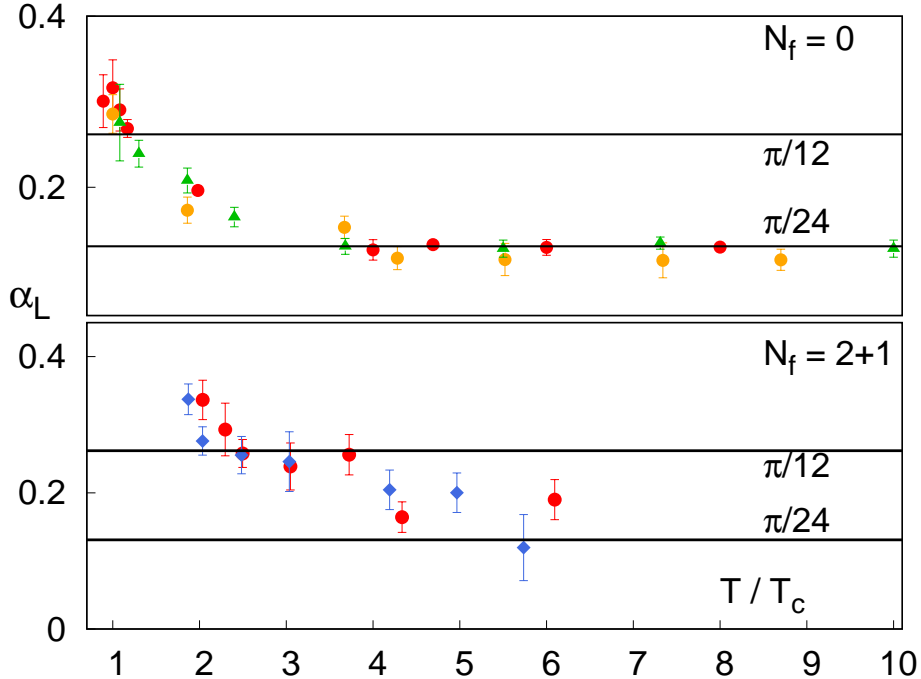


Fig. 1: The coefficient of the Coulomb term extracted from the fit to $V(r)$ at intermediate distances $(\pi T)^{-1} < r < (g^2 T/\pi)^{-1}$ for $N_f = 0$ and $N_f = 2 + 1$ flavor QCD for a range of temperatures between 1-10 T_c . The red, blue, orange and green points correspond to lattice size $N_\tau = 8, 10, 12, 16$ respectively.

The expectation values are calculated typically over 200-2400 gauge configurations in QCD with and without dynamical fermions, details of which are mentioned in the supplementary material. Due to finite statistics the right side of Eq. 1 is dominated by the gauge noise for large distances $L > 5-10$ due to which a clear plateau-like feature is not visible in this observable. This is due to finite lattice size as well as contamination from the excited states. Hence we use an ansatz $m(L, R) = V(R) + b \cdot e^{-V_1 \cdot L}$ in order to extract the ground state energy $V(R)$ reliably at each R by removing the contamination due to the first excited state energy V_1 . We have varied the fit range between $L \in [1, 4]$ for $T \lesssim 4 T_c$ and $L \in [1, 8]$ at $T \gtrsim 4 T_c$. The pseudo-potential is extracted for each jack-knife bin and the statistical errors are estimated from the variance among such bins. For the highest temperatures we have studied, the spatial volumes are small leading to contamination from the excited states leading to larger errors in the extracted pseudo-potential.

The pseudo-potential $V(R)$ has an additional divergence in the continuum due to the self energy of quark and anti-quark pair. We have renormalized $V(R)$ using the same renor-

malization factor (C_Q) [36] which is extracted from the static potential between a quark-antiquark pair at $T = 0$. This is allowed since no new ultraviolet divergences appear at finite temperatures. Further details on our procedure to extract the pseudo-potential and the results for pseudo-potentials at different temperatures and lattice sizes are shown in Fig. 6 and discussed in the supplementary material.

Spatial string tension & the onset of dimensional reduction: Once the renormalized pseudo-potential is measured, we extract the spatial string tension using the ansatz $V(r) = V_0 + \sigma_s r - \alpha_c/r$. We also extract the coupling α_c as a result of the fit. The Coulomb term in the above ansatz could have two possible origins. It could come from the short distance perturbative part, in which case we have $\alpha_c = \alpha_P = (4/3)g^2/(4\pi)$ at leading order. Alternatively, the Coulomb term can arise from the fluctuations of the color flux tube along the transverse direction [37–40], in which case $\alpha_c = \alpha_L = (D - 2)\frac{\pi}{24}$, with D being the spacetime dimension. This is the so-called Lüscher term and the above description applies at relatively large distances. When dimensional reduction sets in $D = 3$, otherwise we have $D = 4$. One would expect that for $r < (\pi T)^{-1}$ the perturbative α_P/r term will dominate the pseudo-potential, whereas for intermediate distances $(\pi T)^{-1} < r < (g^2 T/\pi)^{-1}$ the Lüscher term determined by α_L will be relevant. At large distances $r > (g^2 T/\pi)^{-1}$, one would expect the largest contribution coming from the term containing σ_s . Indeed we observe that the α_c extracted from our fits are close to α_L at intermediate distances $r.T \in [0.5, 1.2]$ and eventually tending towards zero at larger distances.

The results for the extracted α_L is compiled in Fig. 1. The average values of α_L are consistent with $\pi/12$ for $T \lesssim 5 T_c$ ($2 T_c$) but beyond $T \gtrsim 5 T_c$ ($3 T_c$), these values approach $\pi/24$ indicating the onset of dimensional reduction beyond this temperature for QCD with (without) dynamical quarks. Henceforth T_c correspond to T_{pc} (T_d) for $SU(3)$ with (without) dynamical quarks. To ensure the robustness of our extraction method for α_L we have compared our results with a previous lattice study [26] in $SU(3)$ gauge theory with $N_f = 0$. We observe a good agreement with the earlier results. However going to finer $N_\tau = 12, 16$ lattice spacings is important to precisely demonstrate that the value of α_L approaches $\pi/24$ at temperatures $T \gtrsim 4 T_c$. From these observations, we thus held the coefficient of $1/r$ term to a fixed value depending upon the temperature and extract $\sqrt{\sigma_s}/T$ from a two-parameter fit to the pseudo-potential for $SU(3)$ gauge theory with and without dynamical quarks as a function of T/T_c , results of which are shown in Fig. 2. We observe that $\sqrt{\sigma_s}/T$ has a strong

temperature dependence for $T < 4 T_c$, beyond which it is mildly dependent of temperature for $N_f = 0$ case, whereas for $N_f = 2 + 1$, a slow variation with T/T_c persist till $\sim 5 T_c$. This coincides with the onset of dimensional reduction and the 3 dimensional effective theory being confining with the scale characterized by $\sqrt{\sigma_s}$.

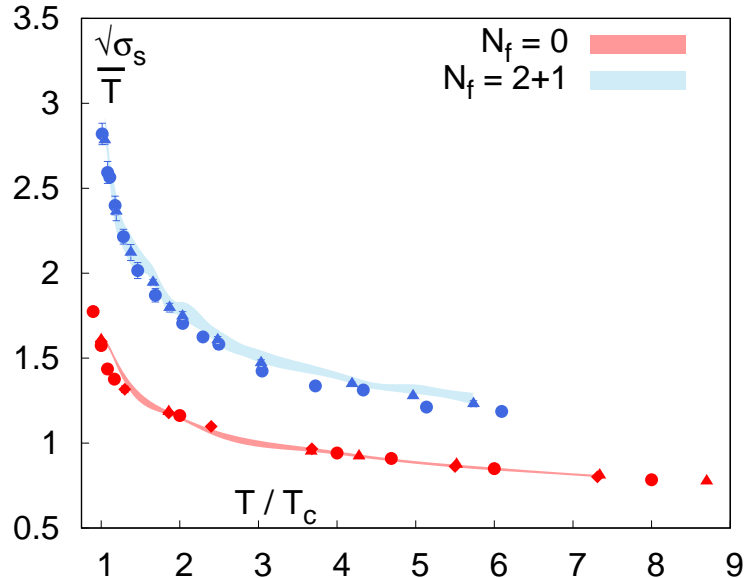


Fig. 2: The comparison of the continuum extrapolated values of $\sqrt{\sigma_s}/T$ as a function of T/T_c for quenched (red band) and 2 + 1 flavor QCD (blue band). The lattice data for cutoff corresponding to $N_\tau = 8, 10, 12, 16$ are shown as circle, triangle, box and diamond symbols respectively.

We next interpret the temperature dependence of the spatial string tension in QCD. The extracted spatial string tension for 2 + 1 flavor QCD, for different lattice spacings or equivalently different $N_\tau = 8, 10$ for the entire temperature range we have studied, is shown in physical units in Fig. 3. The data for $\sqrt{\sigma_s}$ do not show a significant lattice cut-off dependence as evident from the good agreement between $N_\tau = 8$ and $N_\tau = 10$ data. Nevertheless we perform a cubic splines interpolation of the data as a function of temperature and for each N_τ and then perform a continuum extrapolation, which is shown as a red band in Fig. 3. We observe that at $T < 260$ MeV the value of $\sqrt{\sigma_s}$ is in excellent agreement with the string tension, $\sqrt{\sigma} = 0.467$ GeV extracted from the temporal Wilson line correlator [34] at $T = 0$ [22]. At temperatures $\gtrsim 260$ MeV the electric scale gT starts to separate from the hard scale πT resulting in the onset of linear temperature dependence of $\sqrt{\sigma_s}$.

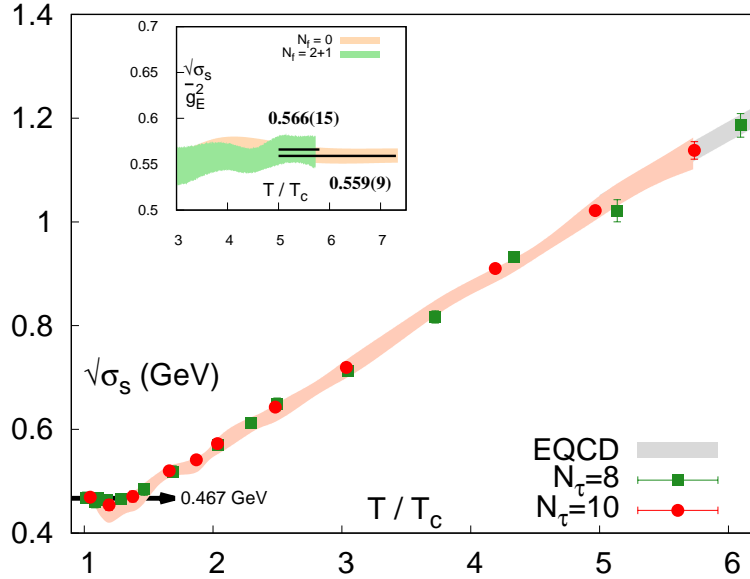


Fig. 3: The variation of $\sqrt{\sigma_s}$ with T/T_c for different lattice cut-offs corresponding to $N_\tau = 8, 10$ along with its continuum estimates (orange band). The continuum estimates are close to EQCD prediction at $T \gtrsim 5 T_c$, shown as gray band. The black line in lower left corner denotes $\sqrt{\sigma} = 0.467$ GeV at $T = 0$ from Ref. [34]. The variation of the continuum estimate for $\sqrt{\sigma_s}/g_E^2$ with T/T_c is shown in the inset for SU(3) (yellow band) and 2+1 flavor QCD (green band) respectively.

At higher temperatures $\sqrt{\sigma_s}$ rises with increasing temperatures and we would like to quantify this trend. To compare with the literature, the variation of $\sqrt{\sigma_s}/g_E^2$ with temperature is shown in the inset of Fig. 3. The 3 dimensional EQCD coupling g_E^2 is calculated up to two-loop in g^2 [41]. It is evident from the plot that the dependence of $\sqrt{\sigma_s}/g_E^2$ on temperature (or equivalently the 4 dimensional gauge coupling g) is mild for $T > 5 T_c$, again reinforcing the validity of an effective 3 dimensional description as also observed in the data for the Lüscher term. The other couplings within EQCD i.e. m_D, λ_E have an even milder dependence on g [41] hence fitting the data for $\sqrt{\sigma_s}/g_E^2$ with a constant function for the range of temperatures between 5-5.8 T_c , we obtain $\sqrt{\sigma_s} = 0.566(15) g_E^2$. Extrapolating our EQCD inspired fit to higher temperatures, shown as a gray band in Fig. 3, we observe that it perfectly accommodates for the lattice data at a cut-off corresponding to $N_\tau = 8, T/T_c \sim 6$, which was not used in the fit. Our results are consistent with the first extensive study in 2+1 flavor QCD performed with a different staggered fermion discretization [27], where

lattice data for $\sqrt{\sigma_s}$ was found to match with $0.54(1)g_E^2$, albeit with a large uncertainty, at temperatures $T \gtrsim 1.5 T_c$ where $T_c \sim 200$ MeV. As already discussed in Ref. [27] major sources of uncertainties in such a direct comparison with the prediction from dimensionally reduced theory are due to errors in the determination of spatial string tension and the coupling g_E in a 3 dimensional SU(3)-Higgs model. We have instead changed the strategy and extracted the dependence of the spatial string tension with g_E^2 with a constant fit to our data for $\sqrt{\sigma_s}/g_E^2$ in a temperature range where we observe hints of the onset of dimensional reduction.

We have also performed the same analysis for SU(3) gauge theory without dynamical quarks but for a wider temperature range, which allows us to observe the onset of dimensional reduction more carefully. Since our continuum extrapolated data for $\sqrt{\sigma_s}/g_E^2$ in SU(3) shows almost no temperature or equivalently the 4 dimensional gauge coupling dependence in the range $5 < T/T_c < 7.3$, hence it can be parametrized as $0.559(9)g_E^2$ in this range and beyond as shown in the inset in Fig. 3. The coefficient which characterizes the variation of $\sqrt{\sigma_s}$ with g_E^2 is in perfect agreement with our observation in 2 + 1 flavor QCD. This confirms the fact that indeed the dynamical fermions do not affect such observables at $T \gtrsim 5T_c$, since it is most sensitive to the magnetic gluons which interact non-perturbatively even at asymptotically high temperatures. Our result agrees with and improves upon the previous lattice study [26] in 4 dimensional SU(3) gauge theory which reported $\sqrt{\sigma_s} = 0.566(13) g_E^2$, where the tree level matching $g_E^2 = g^2(T)T$ was used in the fit but no continuum extrapolation was carried out.

Within 3 dimensional SU(3) gauge theory characterized by a coupling g_3 , two independent lattice studies have reported the variation of $\sqrt{\sigma_s}$ as $\sim 0.553(2)g_3^2$ [42] and $\sim 0.554(4)g_3^2$ [25] whereas a Hamiltonian-based approach in [43] parametrized it as $\sim 0.564 g_3^2$. In the temperature range $5 < T/T_c < 7.3$ we find that for $N_f = 0$ case, the $\sqrt{\sigma_s}/g_3^2 = 0.557(7)$ has no noticeable dependence on temperature, which also alludes to the onset of dimensional reduction. Here we have taken $g_3^2 = g^2T$. We would similarly expect that the MQCD effective theory will start to describe the 2+1 flavor QCD data at these high temperatures as well.

Consequences: Screening mass at high temperatures Having established the non-perturbative nature of the spatial Wilson line correlators and the associated pseudo-potential and determined the value of the spatial string tension the next question we ask is what are the corresponding consequences? In order to address this question one has to choose observables which are most sensitive to the magnetic scale. One of them is the spatial

screening mass of hadron-like excitations [44]. The screening correlators correspond to the long-wavelength or equivalently low-frequency modes of the high-temperature QCD plasma hence should be sensitive to the non-perturbative effects at the magnetic scale. The continuum extrapolated spatial screening mass of pseudo-scalar iso-triplet meson-like excitations in $2 + 1$ flavor QCD measured using HISQ discretization shows a significant deviation from the perturbative EQCD prediction [29] at $T \lesssim 1$ GeV [45–47] and more recently this deviation is observed to persist even at $T \lesssim 164$ GeV [48]. More interestingly there exist a clear difference in the magnitude of the vector and pseudo-scalar meson screening masses at such high temperatures [48] which cannot be explained within the EQCD effective theory at $\mathcal{O}(g^2)$.

In an attempt to understand these puzzles, we recall that at high enough temperatures quark excitations acquire an effective mass $M = \pi T + g^2 T C_F / 8\pi + \mathcal{O}(g^4)$, and the spatial correlation function represent non-relativistic bound states of these heavy quarks in $2 + 1$ dimensions. The screening mass can thus be determined from the lowest eigenvalue of a two dimensional Schrödinger equation with a static potential which until now, has been derived from a systematic $1/(\pi T)$ expansion of the heavy quark propagator in presence of magnetic gluons by resumming gluon-exchange ladder diagrams within EQCD [29]. In order to include the effects of non-perturbatively interacting magnetic gluons we propose a more general procedure to determine the potential by matching to the perturbative potential in the region $r < m_D^{-1}$ to the continuum extrapolated potential $V(r)$ extracted in the previous section at $r \sim m_D^{-1}$. Further details of this matching procedure can be found in supplementary material. The non-perturbative interactions also affect the effective mass M . Hence we determine them by fitting the screening mass $2M + \delta m_{\text{scr}}$ obtained by solving the Schrödinger equation for the zero angular momentum state,

$$\left[-\frac{1}{M} \left(\frac{d^2}{dr^2} + \frac{1}{r} \frac{d}{dr} \right) + V(r) \right] \psi_0(r) = \delta m_{\text{scr}} \psi_0(r) \quad (2)$$

for different trial values of M , to the lattice data on the spin-averaged values of the continuum extrapolated screening mass in $2 + 1$ flavor QCD [48] in the temperature range $T \in [1, 164]$ GeV. This is necessary due to the fact that the pseudo-scalar and vector screening masses are not degenerate, and split evenly due to spin-spin interaction [49, 50] between a heavy quark-antiquark pair which we will derive within the NRQCD framework starting from EQCD Lagrangian. The results for $M/(\pi T)$ as a function of g^2 is shown in

Fig. 4 which we could parametrize using $M/(\pi T) = 1 + 0.0159(15)g^2 - 0.0165(10)g^4$ with a $\chi^2/\text{d.o.f} = 0.53$. The coupling g was estimated at the scale $2\pi T$ using the five-loop beta function with $\Lambda_{\overline{\text{MS}}}^{(3)} = 0.339(12)$. The coefficient of the $\mathcal{O}(g^2)$ term is consistent with the perturbative estimate (0.01688) [29] but non-perturbative interactions which contribute at $\mathcal{O}(g^4)$ is also of the same magnitude with opposite sign. At asymptotically high temperatures M goes over to πT as expected.

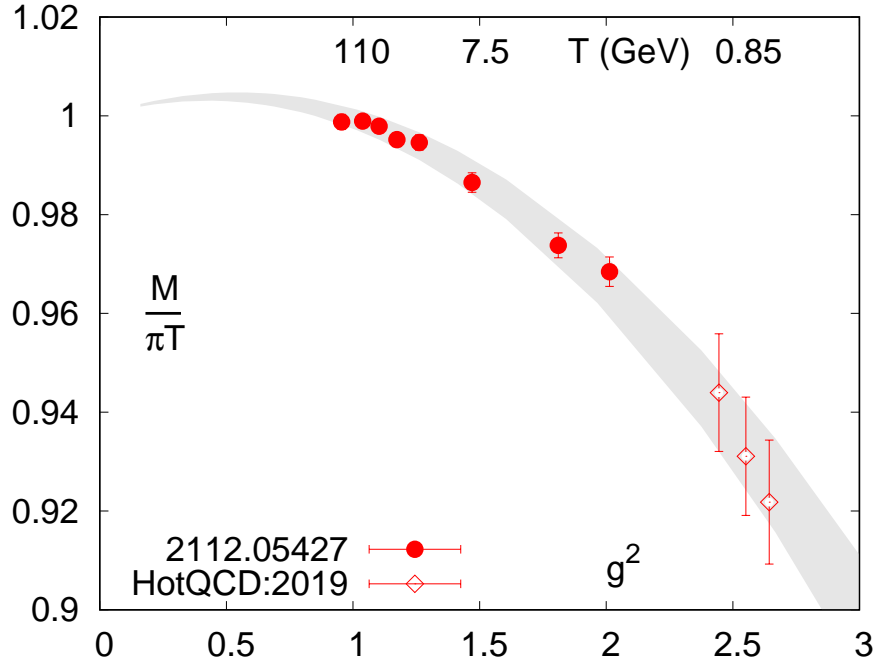


Fig. 4: The results for the mass M that goes into Eq. 2, obtained by performing a fit to the spin-averaged data for screening mass from Ref. [48] at $T \in [1, 164]$ GeV (filled points). The fit extrapolated to lower values of temperature provides a good match to the lattice data (open points) from Ref. [45].

To check the robustness of our procedure we have used this parametrization to estimate spin-averaged screening masses temperatures lower than 1 GeV, which are in good agreement with available lattice QCD results [45] upto $T \gtrsim 5T_c$, where we earlier observed the onset of dimensional reduction. We have also derived the spin dependent potential, $V_s(r) = (\pm \frac{1}{4}) \frac{4g^2 T}{3M^2} \delta^2(r)$ for vector and pseudo-scalar states respectively at $\mathcal{O}(g^2)$, details of which are given in supplementary material. Since this term is subdominant compared to our matched potential $V(r)$, one can treat it as a perturbation. This leads to a correction to the ground state energy of Eq. 2 given by an amount $\delta m_{\text{scr}}^{(1)}(T) = (\pm \frac{1}{4}) \frac{2}{3\pi} \frac{g^2 T}{M^2} |\psi_0(0)|^2$,

for vector and pseudo-scalar states respectively, and depends on the ground state wave function ψ_0 at the origin. We could then estimate the corresponding screening mass $2M + \delta m_{\text{scr}}(T) + \delta m_{\text{scr}}^{(1)}(T)$ normalized by $2\pi T$, which is shown in Fig. 5. Our calculated values are in excellent agreement with the lattice QCD data [45, 51], within 1σ at $T \gtrsim 5T_c$, but more importantly the correct g^2 dependence is achieved over a large temperature range which could not be explained earlier. At lower temperatures, where dimensional reduction is not valid, we do not expect this spin potential to accurately describe the data.

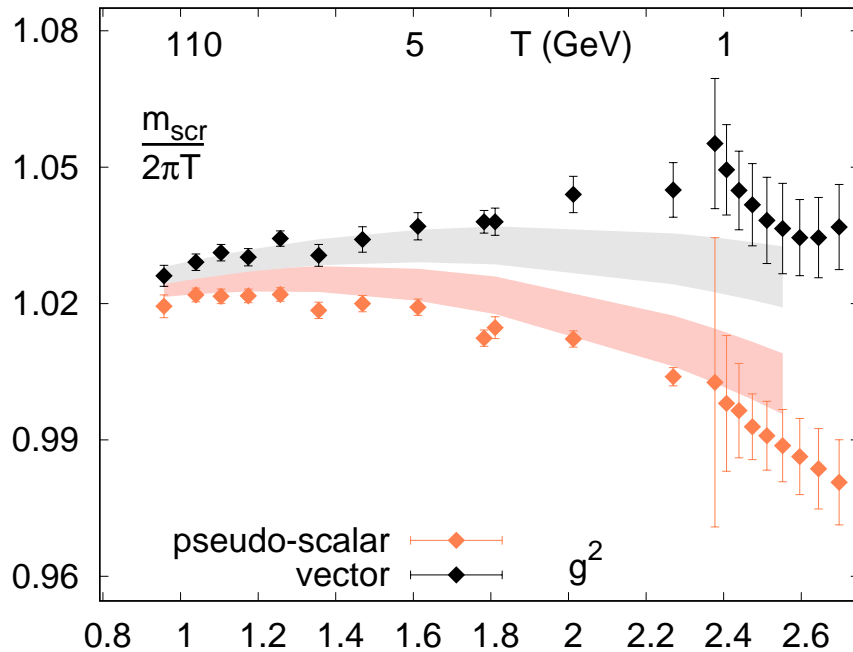


Fig. 5: The splitting between the pseudo-scalar and vector screening masses, shown as red and gray bands respectively, predicted using the spin-spin interaction term derived perturbatively. Our results are compared with lattice QCD data from Refs. [45, 51]. The bands were drawn by performing a simple interpolation of the data points in the entire range of temperatures $\gtrsim 5 T_c$.

Summary & Outlook: In this Letter, we explain an important feature of the strongly interacting quark gluon plasma i.e. the deviation of the screening mass corresponding to the long-wavelength excitations of the plasma from its perturbative EQCD prediction by including non-perturbative interactions of the magnetic gluons quantified by the spatial string tension. By performing a careful continuum extrapolation of $\sqrt{\sigma_s}$ and studying its temperature dependence we estimate the temperature regime $T \gtrsim 5T_c$ where QCD can be

described by a dimensionally reduced effective theory. In this regime we calculate the *effective* potential that enters into the determination of the screening masses by matching the non-perturbative potential (at long distances) with the EQCD potential (valid at short distances) at the Debye scale. Remarkably the ground state wave function obtained using this potential can be used to explain the spin-splitting that exist between the pseudo-scalar and vector screening masses for a wide range of temperatures up to $T \gtrsim 5T_c$, without any additional parameter tuning. As a followup we will like to extend our formalism to explain the large spin-splitting that persist in the screening masses in QCD closer to T_c and further quantify how non-perturbative interactions at the magnetic scale enter into transport properties of the quark-gluon plasma. Another interesting direction will be to generalize our formalism to predict baryon screening masses [52].

Acknowledgements This work was supported by the Deutsche Forschungsgemeinschaft (DFG, German Research Foundation) Proj. No. 315477589-TRR 211 and the U.S. Department of Energy, Office of Science, through Contract No. DE-SC0012704. Computations have been performed on the GPU Cluster at Bielefeld University and at the Institute of Mathematical Sciences. Part of the HISQ calculations were performed using the SIMULATEQCD [53] library.

APPENDIX

A. Details of the Lattice methodology

The spatial Wilson line correlators in $2 + 1$ flavor QCD at finite temperatures, are measured on the gauge configurations which were generated by HotQCD collaboration to study QCD equation of state and quark number susceptibilities [31–33, 54] using physical strange quark mass and light quark mass $m_l = m_s/20$ such that the Goldstone pion mass is 160 MeV. These gauge configurations were generated using RHMC algorithm with highly improved staggered quarks action (HISQ) for the fermions [55, 56] and Symanzik improved gauge action. The correlators are calculated on configurations which are separated by 10 RHMC steps. The choice of HISQ discretization ensures that finite cut-off and taste-splitting effects [57] are optimized even on a finite lattice. The lattice used in this study has a spatial volume N^3 and number of sites along the Euclidean time direction to be N_τ satisfying

$N/N_\tau = 4$ which ensures that finite volume effects are minimal. The temperature is denoted as $T = 1/(N_\tau a)$ hence at each temperature we have performed our measurements on $N_\tau = 8, 10$ lattice in order to perform a continuum extrapolation of the spatial string tension extracted out of the spatial Wilson line correlators. The measurements are performed over a wide range of temperatures from 0.166(0.168)-1(0.924) GeV for $N_\tau = 8$ (10) respectively and the typical lattice spacing ranges from 0.15 fm to 0.04 fm. The complete list of parameters used in our work are listed in Table I. We have also performed the calculation of the spatial string tension on quenched SU(3) gauge configurations which are generated using the standard Wilson gauge action with heat-bath updates and 4 over-relaxation steps per update. The typical lattice extents along the spatial direction are chosen to $N = 32, 48, 64$ and the corresponding $N_\tau = 8, 12, 16$ for different $\beta = 6/g_0^2$ values corresponding to the bare gauge coupling g_0 . The temperature corresponding to each lattice spacing has been calculated in terms of the Sommer parameter r_0/a whose parametrization in terms of β has been taken from Ref. [5].

B. Details of the procedure to measure the Pseudo-potential and gauge-fixing

To extract the color-singlet pseudo-potential between a infinitely massive, static $q\bar{q}$ pair separated by distance r we have defined the two-point spatial Wilson line correlator as,

$$W(r, l)_{\vec{x}_\perp, z} \equiv \frac{1}{3} \mathbf{Tr}_c [S_z(\vec{x}_\perp, l) S_z^\dagger(\vec{x}_\perp + \vec{r}, l)] \quad , \quad (3)$$

where $S_z(\vec{x}_\perp, \tau, l) = \exp\left(i \int_z^{\tau+l} dz A_z(\vec{x}_\perp, z, \tau)\right)$ is the spatial Wilson line along the z direction of length $l = La$ which are separated by a distance $r = Ra$ in the x - y plane at all possible initial z sites and on each τ slices. The \mathbf{Tr}_c denotes trace over the color space. All possible such correlators consisting of Wilson lines of length L separated by R are measured and the average over these different sizes is denoted by $W(R, L)$. As the gauge noise present in the correlators defined at large R, L is typically large, we have only taken into account $R, L \leq N/2(N/4)$ for on(off)-axis correlators.

The static potential between a static quark-antiquark pair has been calculated using temporal Wilson line correlators at zero temperature in a gauge-invariant manner in Ref. [58, 59]. In this calculation one has to choose a gauge which is local in the Euclidean time such that the eigenspectrum of the transfer matrix remains exactly the same as for the gauge

β	$N_\tau = 8$			$N_\tau = 10$		
	T(MeV)	N_{conf}	σ_s/T^2	T(MeV)	N_{conf}	σ_s/T^2
6.423	166.6	1700	7.95(36)			
6.488	177.5	1700	6.72(33)			
6.515	182.2	1700	6.58(11)			
6.575	193.3	1700	5.75(26)			
6.664	210.7	1090	4.91(19)	168.6	1071	7.75(14)
6.800	240.3	1670	4.06(19)	192.2	1835	5.59(26)
6.950	277.2	2400	3.50(15)	221.8	1317	4.50(20)
7.150	334.2	850	2.90(4)	267.4	1014	3.78(7)
7.280	376.6	270	2.64(6)	301.3	828	3.23(9)
7.373	409.7	500	2.50(9)	327.8	869	3.05(9)
7.596	500.0	500	2.03(5)	400.0	672	2.58(6)
7.825	611.1	500	1.79(5)	488.9	717	2.17(6)
8.000	711	1830	1.72(3)			
8.200	843	249	1.47(6)	675	900	1.82(3)
8.400	1000	249	1.41(5)	800	750	1.63(3)
8.570				924	200	1.52(4)

Tab. I: The parameters for the lattice calculations in 2 + 1 flavor QCD for two different $N_\tau = 8, 10$ and the values of the spatial string tension σ_s/T^2 at each temperature.

invariant Wilson loop of the same size. Some of the possible gauge choices discussed are the Coulomb gauge and Laplacian Coulomb gauge. Typically, when determining the equation of state [60, 61] the temperature is set in terms of a scale r_0, r_1 which are extracted from the static potential in terms of temporal Wilson line correlators in the Coulomb gauge. In our case, we are calculating two-point spatial Wilson line correlator in the z direction, hence the choice of gauge should be such that it is local in the z direction to preserve the eigenstates of the spatial transfer matrix. We have chosen a modified-Coulomb gauge, which in the continuum limit is given by $\partial_x A_x + \partial_y A_y + \partial_\tau A_\tau = 0$.

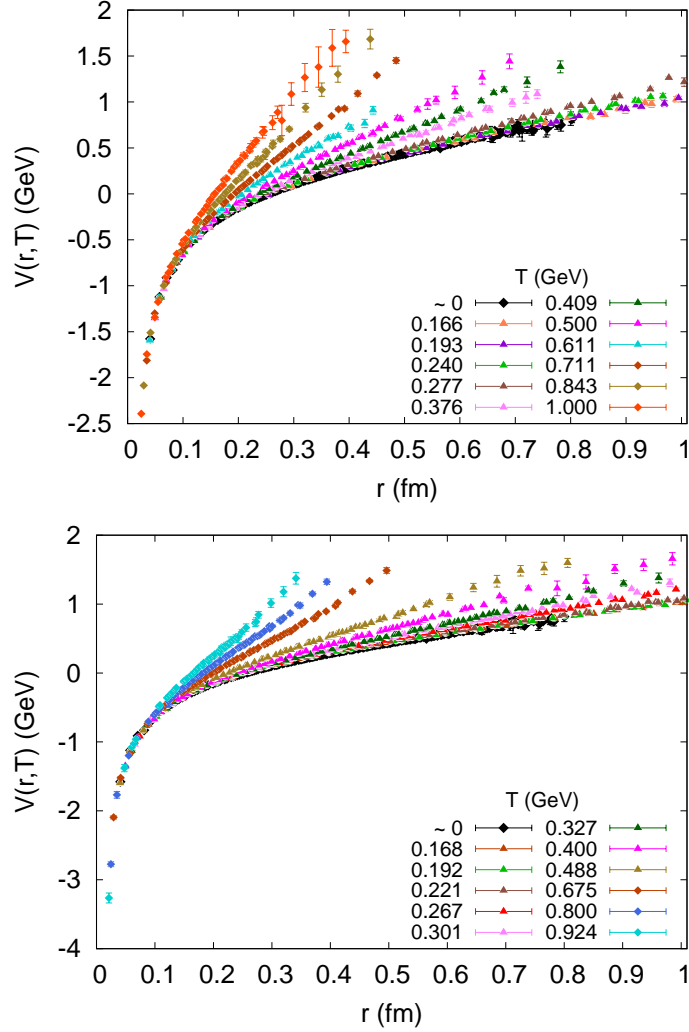


Fig. 6: The pseudo-potential $V(r, T)$ for 2 + 1 flavor QCD as a function of r at two lattice cut-offs corresponding to $N_\tau = 8, 10$ is shown in the top and bottom panels respectively. The temperature ranges from 166-1000 (168 – 924) MeV for $N_\tau = 8$ (10). We have compared our data with zero temperature potential denoted by black points, taken from Ref. [34].

We have implemented the gauge-fixing procedure as outlined in Ref. [51]. We extract the ground state energy out of the eigenvalues of the spatial Hamiltonian which in the limit $L \rightarrow \infty$ gives us the pseudo-potential representing the interaction between a quark and the antiquark like excitations in addition to their self energies.

The results for $V(r, T)$ in physical units as a function of distance r is shown in Fig. 6 for different temperatures for 2+1 flavor QCD and is compared to the zero temperature potential extracted earlier from Ref. [34]. It is clearly evident that the pseudo-potential do not vary

with increasing temperatures up to about $T \approx 260$ MeV, and this is independent of the lattice cut-off. Further the dependence of $V(r, T)$ as a function of r is very similar to the zero temperature potential extracted from the temporal Wilson line correlators. Beyond $T \gtrsim 260$ MeV the pseudo-potential rises more steeply as a function of r with increasing temperatures. Above 260 MeV, the hard and the electric scales $\pi T, gT$ just start to separate out, which is the reason behind the observable temperature dependence of the pseudo-potential. At the largest temperatures we have studied so-far the maximum extent of the box becomes small since the lattice spacing decreases. The finite volume effects at large distances are clearly visible resulting in a kink-like feature in $V(r, T)$ at the highest temperatures, where we could reliably measure them. This is a characteristic feature arising from contamination of the ground state energy due to higher excited states. We have observed this while extracting the pseudo-potential by varying the L_{\min} while performing a fit to the $m(L, R)$. However large errors in the data at large R does not allow us to precisely determine the excited state contribution. We have not shown the pseudo-potentials for quenched QCD since the renormalization factor is not available in the literature.

C. Details of the procedure to extract α_L & σ_s

Within the dimensionally reduced effective theory of QCD, $\sqrt{\sigma_s}$ increases linearly with temperature which also results in the increasing slope of the pseudo-potential with temperature at large distances, evident in Fig. 6. At first, we have extracted the coefficient of the $1/r$ term using the ansatz $V(r) = V_0 + \sigma_s r - \alpha_c/r$ over a range of values of $r \in [r_{\min} : r_{\max}]$. Our strategy is to study the variation of α_c as a function of r_{\min} . In this Cornell-like fit, the perturbative Coulomb contribution at $r < (\pi T)^{-1}$ is expected to be sub-dominant at distances $r > (gT)^{-1}$, where the Lüscher term with strength α_L will start to be important and will eventually be taken over by the string tension term at $r > (g^2 T/\pi)^{-1}$. We have observed that the α_c extracted from the fit decreases with increasing r_{\min} , where we have kept $r_{\min} \cdot T = 1$. The value of α_c varies from its perturbative value α_P at $r < (\pi T)^{-1}$ to α_L in the intermediate distances and eventually falling to zero at large distances $r \gtrsim (g^2 T/\pi)^{-1}$. We have thus extracted α_L by varying our r_{\min} in the range between $(\pi T)^{-1} - (g^2 T/\pi)^{-1}$ for both quenched QCD and 2 + 1-flavor QCD at different temperatures. The values of the α_L as a function of T/T_c are shown in Fig. 1. However extraction of α_L with our procedure

is not possible for temperatures $T \lesssim 2 T_c$ as the scales are not well separated enough.

Even though the coefficient of the $1/r$ term goes to zero at large distances the extraction of σ_s from a 3 parameter Cornell-like fit is not very stable. Hence we set $r_{\min} > (gT)^{-1}$ and fixed the co-efficient of the $1/r$ term to i) $\alpha = \pi/12$ or ii) $\alpha = \pi/24$ according to the temperature where we are performing the fit and extract σ_s from a two parameter fit. To verify the robustness of our procedure we have checked that the extracted σ_s is stable with the variation of r_{\min} used in the fit. For low temperatures $T < 4 T_c(1.5 T_c)$, the σ_s is extracted from the two parameter fit keeping $\alpha_L = \pi/12$ agrees with the Cornell-like fit value within $1-\sigma$. At higher temperatures i.e. $T > 5 T_c(4 T_c)$, the σ_s is obtained from a two parameter fit keeping $\alpha_L = \pi/24$ fixed and it saturates to a constant value which also agrees to that obtained from the Cornell-like fit within $1-\sigma$. This observation points toward the onset of dimensionally reduced effective theory description of QCD, both with and without dynamical fermions. The saturation in the extracted values of σ_s to a stable value at large r_{\min} is even more evident for quenched QCD than in $2 + 1$ flavor QCD, where our statistics are higher. We have not considered the logarithm in r perturbative potential at short distances while performing the fits to the high temperature data, which would arise in 3 dimensions, as we cannot distinguish it from the Coulomb potential within our statistics.

D. Details of matching procedure of $V(R)$ with the EQCD inspired potential

At high enough temperatures where the scales in thermal QCD are well separated i.e. $\pi T \gg gT$, such the Euclidean temporal extent is infinitesimally small the A_0 fields become static and QCD can be described in terms of an effective theory consisting of dynamical gauge fields $A_i(\vec{x})$, $i \in [1, 3]$ coupled to adjoint scalar fields $A_0(\vec{x})$ and is known as EQCD [12, 16]. The EQCD action in Euclidean space,

$$S_{\text{EQCD}} = \int d^3x \left[\frac{1}{4} \bar{F}_{ij}^a \bar{F}_{ij}^a + \text{Tr}([\bar{D}_i, \bar{A}_4][\bar{D}_i, \bar{A}_4]) + m_D^2 \text{Tr}(\bar{A}_4^2) + \lambda_E (\text{Tr}(\bar{A}_4^2))^2 + \dots \right], \quad (4)$$

can be written in terms of the low energy coefficients, the Debye mass m_D and couplings g_E, λ_E which at two loop in g [41] are

$$g_E^2 = g^2 T \left[1 + \frac{g^2}{(4\pi)^2} \alpha_{E7} + \frac{g^4}{(4\pi)^4} \gamma_{E1} + \mathcal{O}(g^6) \right] \quad (5)$$

$$m_D^2 = g^2 T^2 \left[\frac{N_c}{3} + \frac{N_f}{6} + \frac{g^2}{(4\pi)^2} \alpha_{E6} + \mathcal{O}(g^4) \right]. \quad (6)$$

In our work the number of flavors is $N_f = 3$ and $N_c = 3$. Note that $D_i = \partial_i - igA_i$, $F_{ij} = \frac{i}{g}[D_i, D_j]$ and the bar denotes fields defined within EQCD. Clearly the EQCD is valid at length scales $r > (\pi T)^{-1}$. Since we are interested in the physics at infrared momentum scales $\lesssim g^2 T/\pi$, the effects of the fermion and gauge fields with non-zero Matsubara frequencies can be integrated out to produce an effective theory of the zero modes. The adjoint scalar fields which acquire a mass $\mathcal{O}(gT)$ at the tree level in the static limit, can be integrated out to an effective theory valid at $r > (g^2 T/\pi)^{-1}$ known as MQCD, which is described by a 3 dimensional pure gauge action without dynamical fermions,

$$S_{\text{MQCD}} = \int d^3x \left(\frac{1}{4} \bar{F}_{ij}^a \bar{F}_{ij}^a + \dots \right), \quad i, j = 1, 2, 3. \quad (7)$$

with a dimensionful coupling g_3 which can be related to the QCD coupling g in 4 dimensions through the following 2-loop relation [62]. When calculating the coupling g_E in the dimensionally reduced theory as a function of g using the Eq. 5, the g is calculated at a scale $\bar{\mu}$ which in the $\overline{\text{MS}}$ scheme is $\bar{\mu}^2 = 4\pi\mu^2 e^{-\gamma_E}$, where γ_E is the Euler-gamma constant and $\alpha_{E6}, \alpha_{E7}, \gamma_{E1}$ depends on $\bar{\mu}/T$. We have used the optimal-scale selection criterion [41] where the scale μ_{opt} is chosen such that the error due to the arbitrariness in the scale setting for the determination of g_E^2 remains minimal. The optimal scale is $\mu_{\text{opt}}/T = 9.082$ and 6.742 , while calculating g_E^2 from g with $\Lambda_{\overline{\text{MS}}}^{(3)} = 0.339(12)$ and $\Lambda_{\overline{\text{MS}}}^{(0)} = 0.261(15)$ [63] respectively in QCD with and without three dynamical fermions. We have used five loop beta function to estimate g at each temperature using the RunDec software [64]. To include all possible sources of errors in the calculation of g_E we have varied $\bar{\mu} \lesssim (0.5, 2) \cdot \mu_{\text{opt}}$ and taken into account the systematic errors due to uncertainties in $\Lambda_{\overline{\text{MS}}}$ and T_c , and the statistical errors in our estimation of $\sqrt{\sigma_s}$ through a bootstrap analysis.

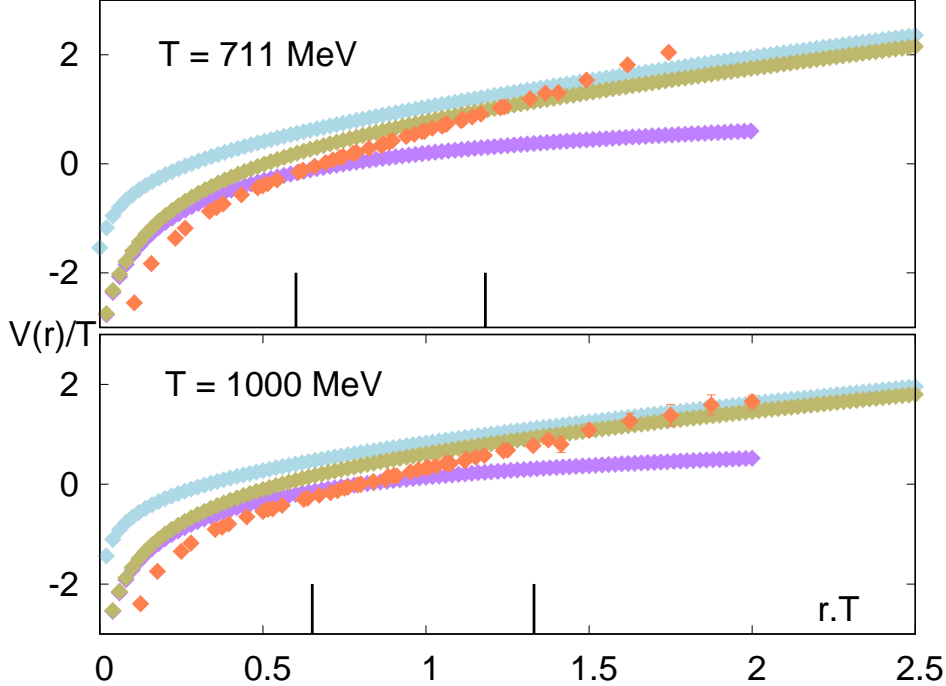


Fig. 7: Comparison of the non-perturbative pseudo-potential $V(r)$ calculated in this work (orange) with the perturbative EQCD potential [41] (purple) and the three dimensional perturbative potential derived in Ref. [65] (light-blue). We have measured the complete potential by matching the EQCD potential with our results for $V(r)$ at the Debye scale given by $r \sim (gT)^{-1}$ (left solid line). The second black line to the right corresponds to non-perturbative magnetic scale $r = (g^2T/\pi)^{-1}$.

Since the EQCD coupling is known from Eq. 6, we can perform a comparison of the spatial string tension calculated by us with the effective theory estimates, which has been discussed at length in the Letter. We now detail the procedure where we determine the most general pseudo-potential at high temperatures, by properly including the perturbative potential derived earlier within the EQCD framework [41] and the non-perturbative part at the large distances encoded by the spatial string tension. Before proceeding we compare the perturbative EQCD potential with the pseudo-potential that we have estimated for 2+1 flavor QCD and also a variant of the potential calculated perturbatively in three dimensions [65]. The result for the comparison is shown in Fig. 7. It is evident from the plot that the non-perturbative pseudo-potential (orange points) differs from the EQCD potential (purple points) at short distances $r \lesssim 1/\pi T$ but matches quite well in the intermediate region $(gT)^{-1} < r < (g^2T/\pi)^{-1}$ and then starts again deviate from each other at

large distances. This emphasizes the importance of non-perturbative effects at length scales larger than $(g^2T/\pi)^{-1}$. The perturbative 3 dimensional potential start to agree with the non-perturbative $V(r)$ at long distances only at very high temperatures $\gtrsim 1$ GeV. However since the ratio of the spatial string tension σ_s measured in this work with/without dynamical fermions versus its perturbative estimate [65] is typically about $\sigma_s/\sigma_{\text{per}}^{N_f=0} = 2.30(2)$ at $T \gtrsim 5T_c$, the full non-perturbative determination of the pseudo-potential is essential to describe the physics of the deep magnetic sector of the quark-gluon plasma. Hence to correctly account for both the short distance perturbative interactions and the non-perturbative interactions at long distance scales we match the pseudo-potential $V(r)$ measured in this work with the EQCD potential at $r \gtrsim 1/m_D$ which is implemented through the relations,

$$\begin{aligned} \frac{V(\hat{r})}{2\pi T} &= \frac{C_F}{(2\pi)^2} \frac{g_E^2}{T} \left[\ln \frac{\hat{r}}{2} + \gamma_E - K_0(\hat{r}) \right], \quad \hat{r} < 1 \\ &= \frac{1}{2\pi} \left[\hat{\sigma}_s \frac{\hat{r}}{\hat{m}_D} - \frac{\pi}{24} \frac{\hat{m}_D}{\hat{r}} \right], \quad \hat{r} \geq 1, \end{aligned} \quad (8)$$

where $\hat{r} \gtrsim r m_D$, $C_F = \frac{N_c^2 - 1}{2N_c}$, $\hat{\sigma}_s = \sigma_s/T^2$, $\hat{m}_D = m_D/T$, γ_E is Euler gamma-constant and $K_0(r)$ is modified Bessel function of 2nd kind. This is done at temperatures $\gtrsim 5T_c$ where the long distance part of the pseudo-potential is effectively described by MQCD.

E. Details of Screening Mass calculation

In the quark gluon plasma phase, color-singlet meson-like spatially correlated states describe the long wavelength plasma excitations [44]. These *screening* correlators can be constructed in different quantum number channels. One can predict the correlation lengths of these states or the corresponding screening masses m_{scr} , by visualizing them as non-relativistic bound states of massive quark-like excitations of mass $\sim \pi T$ [50] which are obtained by solving for the ground state of the Schrödinger equation,

$$\left[-\frac{\hat{m}_D^2}{2\pi^2 x} \left(\frac{d^2}{d\hat{r}^2} + \frac{1}{\hat{r}} \frac{d}{d\hat{r}} \right) + \frac{V(\hat{r})}{2\pi T} \right] \hat{\psi}_0(\hat{r}) = \frac{\delta m_{\text{scr}}}{2\pi T} \hat{\psi}_0(\hat{r}) \quad (9)$$

written in terms of a dimensionless variable $\hat{r} = m_D r$ and a constant term $x = M/(\pi T)$. The ground state wave function is also normalized in units of m_D , $\hat{\psi}_0(\hat{r}) = \psi_0(\hat{r})/m_D$ and the mass that enters in this calculation has to be appropriately renormalized. The renormalized mass has been calculated within EQCD [29] as $M = \pi T + \frac{g^2 T}{8\pi} C_F + \mathcal{O}(g^4 T)$. The typical

potential $V(r)$ that enters into the calculations is usually derived perturbatively in EQCD where the parameters g_E^2, m_P^2, M are calculated upto $\mathcal{O}(g^2)$ [29].

In this work we have instead, used the potential calculated through our matching procedure discussed in the previous section in determining the screening mass. We also follow a different strategy, where we vary the input M while solving for Eq. 9 such that the bound state energy $2M + \delta m_{\text{scr}}$ thus obtained, agrees with the lattice QCD determination of spin-averaged meson screening masses in 2+1 flavor QCD at each temperature in the range from $T \approx 1-164$ GeV [48]. The spin-averaging has been done by averaging over the pseudo-scalar and vector screening mass since we will show in the next section that spin-dependent potential acts with equal magnitude but opposite signs between these states. After extracting the M for these massive excitations, we have parametrized $M/(\pi T)$ with an ansatz $1 + c_1 g^2 + c_2 g^4$, where the coefficient of g^4 term is a purely non-perturbative contribution, not studied earlier. Next using this parametrization of M , we have solved the Schrödinger equation for a new range of temperatures $T \leq 1$ GeV and matched the ground state energy with the spin-averaged lattice QCD data for screening masses from Ref. [45]. We find an excellent agreement upto temperatures as low as $5 T_c$ ensuring the robustness of our procedure. Further we have explained the splitting that exist between the pseudo-scalar and vector screening masses which cannot be explained within the perturbative EQCD calculations. We will outline the derivation of the spin-spin interaction potential starting from a 2 + 1-dimensional NRQCD Lagrangian, in the next section.

F. Derivation of spin dependent potential

We start from the EQCD gauge fields whose Lagrangian in 2 + 1 dimensions is given in Eq. 4 and introduce heavy fermion-like excitations with an effective mass M . Using non-relativistic approximation i.e. expanding in powers of $\mathcal{O}(1/M)$ [29] one obtains the NRQCD Lagrangian that denotes the dynamics of a fermion-like excitations. The effective Lagrangian in terms of two component spinors $\chi(\phi)$ is

$$\begin{aligned} \mathcal{L}_E^f &= i\chi^\dagger \left[M - gA_0 + D_3 - \frac{1}{2M} (D_k^2 - ig[s_k, s_l]F_{kl}) \right] \chi \\ &+ i\phi^\dagger \left[M - gA_0 - D_3 - \frac{1}{2M} (D_k^2 - ig[s_k, s_l]F_{kl}) \right] \phi . \end{aligned}$$

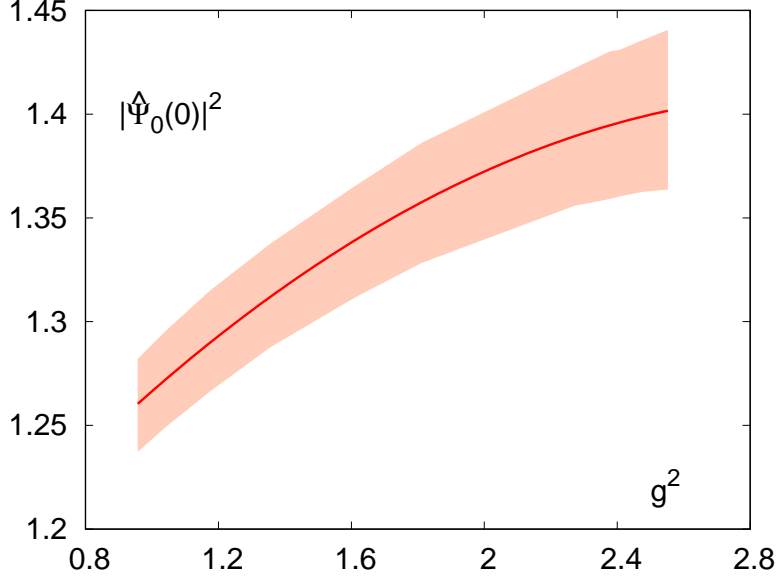


Fig. 8: The probability density of the ground-state wave function representing a screening state at the origin can be parametrized as $|\hat{\psi}_0(0)|^2 = 1.092(2) + 0.208(3)g^2 - 0.0340(9)g^4$ within our non-perturbative treatment of the Schrödinger equation given in Eq. 9.

In the EQCD Lagrangian gauge fields have mass dimension half after rescaling with $T^{1/2}$ whereas in the above Lagrangian it is unity. The spinor fields with spin $s_k \equiv \sigma_k/2$, labeled by the index $k = 1, 2$, where σ_k are the Pauli matrices, are separated by a distance $r_\perp = |\vec{x}_{1\perp} - \vec{x}_{2\perp}|$ and evolves along the z direction from $z = -\frac{L}{2}$ to $z = \frac{L}{2}$. The quantum state of this system can be constructed out of the vacuum $|\Omega\rangle$, which is

$$|\psi(z)\rangle \equiv \chi_\beta^\dagger(\vec{x}_{1\perp}, z) \Gamma^{\beta\alpha} U^\dagger(z, \vec{x}_{1\perp}, \vec{x}_{2\perp}) \phi_\alpha(\vec{x}_{2\perp}, z) |\Omega\rangle$$

The Γ matrix determines the quantum number of the meson-like channel we want to consider. The static potential corresponding to the spin-spin interaction can be extracted from the leading order term of the amplitude $\langle \psi(\frac{L}{2}) | \psi(-\frac{L}{2}) \rangle$ that follows an exponential fall-off at large L . Using a perturbative expansion in orders of g we can calculate this amplitude in the path integral method recovering the EQCD potential in Eq. 8.

The amplitude can be calculated to be

$$\begin{aligned} & \langle \psi\left(\frac{L}{2}\right) | \psi\left(-\frac{L}{2}\right) \rangle \xrightarrow{L \rightarrow \infty} 2 \exp[-2ML \\ & + V(r_\perp)L - \frac{g^2 T C_F L}{2M^2} \text{Tr}[\Gamma(s_1)_z \Gamma(s_2)_z] \delta^2(r_\perp)] \end{aligned} \quad (10)$$

For the pseudo-scalar ($\Gamma \equiv \sigma_3$) and vector channels ($\Gamma \equiv \sigma_{1,2}$) the potential turns out to be $V(r_\perp) \mp \frac{g^2 \text{TCF}}{M^2} \frac{1}{4} \delta^2(r_\perp)$ respectively, denoting the contribution due to spin-spin interaction.

A similar form of the spin-splitting potential was discussed earlier with different coefficients for pseudo-scalar and vector channel in ref. [50] but our formalism is more general. Since this term V_s is subdominant compared to $V(r)$ already used for solving the Schrödinger equation, we can treat it as a perturbation. We have also measured the strength of the bound state wave function (normalized by the Debye mass), at the origin $|\hat{\psi}_0(0)|^2$ for different temperatures or equivalently the gauge couplings g shown in Fig. 8. We observe that the strength increases at higher couplings or equivalently lower temperatures, thus increasing the spin-splitting i.e. the difference between pseudo-scalar and vector screening masses, which is also evident in the lattice QCD data.

-
- [1] D. J. Gross, R. D. Pisarski, and L. G. Yaffe, *Rev. Mod. Phys.* **53**, 43 (1981).
 - [2] E. V. Shuryak, *Rev. Mod. Phys.* **65**, 1 (1993).
 - [3] G. Boyd, J. Engels, F. Karsch, E. Laermann, C. Legeland, M. Lutgemeier, and B. Petersson, *Phys. Rev. Lett.* **75**, 4169 (1995), arXiv:hep-lat/9506025.
 - [4] Y. Aoki, G. Endrodi, Z. Fodor, S. D. Katz, and K. K. Szabo, *Nature* **443**, 675 (2006), arXiv:hep-lat/0611014.
 - [5] A. Francis, O. Kaczmarek, M. Laine, T. Neuhaus, and H. Ohno, *Phys. Rev. D* **91**, 096002 (2015), arXiv:1503.05652 [hep-lat].
 - [6] A. Bazavov, H.-T. Ding, P. Hegde, O. Kaczmarek, F. Karsch, N. Karthik, E. Laermann, A. Lahiri, R. Larsen, S.-T. Li, S. Mukherjee, H. Ohno, P. Petreczky, H. Sandmeyer, C. Schmidt, S. Sharma, and P. Steinbrecher, *Physics Letters B* **795**, 15–21 (2019).
 - [7] F. Burger, E.-M. Ilgenfritz, M. P. Lombardo, and A. Trunin, *Phys. Rev. D* **98**, 094501 (2018), arXiv:1805.06001 [hep-lat].
 - [8] S. Borsanyi, Z. Fodor, J. N. Guenther, R. Kara, S. D. Katz, P. Parotto, A. Pasztor, C. Ratti, and K. K. Szabo, *Phys. Rev. Lett.* **125**, 052001 (2020), arXiv:2002.02821 [hep-lat].
 - [9] R. V. Gavai, M. E. Jaensch, O. Kaczmarek, F. Karsch, M. Sarkar, R. Shanker, S. Sharma, S. Sharma, and T. Ueding, (2024), arXiv:2411.10217 [hep-lat].
 - [10] T. Appelquist and J. Carazzone, *Phys. Rev. D* **11**, 2856 (1975).

- [11] S. Nadkarni, Phys. Rev. D **27**, 917 (1983).
- [12] E. Braaten and A. Nieto, Phys. Rev. D **53**, 3421 (1996), arXiv:hep-ph/9510408.
- [13] K. Kajantie, M. Laine, K. Rummukainen, and M. E. Shaposhnikov, Nucl. Phys. B **503**, 357 (1997), arXiv:hep-ph/9704416.
- [14] F. Karsch, M. Oevers, and P. Petreczky, Phys. Lett. B **442**, 291 (1998), arXiv:hep-lat/9807035.
- [15] A. D. Linde, Phys. Lett. B **96**, 289 (1980).
- [16] T. Appelquist and R. D. Pisarski, Phys. Rev. D **23**, 2305 (1981).
- [17] E. D'Hoker, Nucl. Phys. B **180**, 341 (1981).
- [18] M. Laine and O. Philipsen, Phys. Lett. B **459**, 259 (1999), arXiv:hep-lat/9905004.
- [19] R. V. Gavai and S. Gupta, Phys. Rev. Lett. **85**, 2068 (2000), arXiv:hep-lat/0004011.
- [20] B. Svetitsky and L. G. Yaffe, Nucl. Phys. B **210**, 423 (1982).
- [21] C. Borgs, Nucl. Phys. B **261**, 455 (1985).
- [22] E. Manousakis and J. Polonyi, Phys. Rev. Lett. **58**, 847 (1987).
- [23] L. Karkkainen, P. Lacock, D. E. Miller, B. Petersson, and T. Reisz, Phys. Lett. B **312**, 173 (1993), arXiv:hep-lat/9306015.
- [24] G. S. Bali, J. Fingberg, U. M. Heller, F. Karsch, and K. Schilling, Phys. Rev. Lett. **71**, 3059 (1993), arXiv:hep-lat/9306024.
- [25] F. Karsch, E. Laermann, and M. Lütgemeier, Physics Letters B **346**, 94–98 (1995).
- [26] G. Boyd, J. Engels, F. Karsch, E. Laermann, C. Legeland, M. Lutgemeier, and B. Petersson, Nucl. Phys. B **469**, 419 (1996), arXiv:hep-lat/9602007.
- [27] M. Cheng *et al.*, Phys. Rev. D **78**, 034506 (2008), arXiv:0806.3264 [hep-lat].
- [28] N. Haque and M. G. Mustafa, Prog. Part. Nucl. Phys. **140**, 104136 (2025), arXiv:2404.08734 [hep-ph].
- [29] M. Laine and M. Vepsäläinen, JHEP **02**, 004 (2004), arXiv:hep-ph/0311268.
- [30] C. Aubin, C. Bernard, C. DeTar, J. Osborn, S. Gottlieb, E. B. Gregory, D. Toussaint, U. M. Heller, J. E. Hetrick, and R. Sugar, Phys. Rev. D **70**, 094505 (2004), arXiv:hep-lat/0402030.
- [31] A. Bazavov *et al.*, Phys. Rev. D **85**, 054503 (2012), arXiv:1111.1710 [hep-lat].
- [32] A. Bazavov *et al.* (HotQCD), Phys. Rev. D **90**, 094503 (2014), arXiv:1407.6387 [hep-lat].
- [33] A. Bazavov, P. Petreczky, and J. H. Weber, Phys. Rev. D **97**, 014510 (2018), arXiv:1710.05024 [hep-lat].
- [34] N. Brambilla, R. L. Delgado, A. S. Kronfeld, V. Leino, P. Petreczky, S. Steinbeißer, A. Vairo,

- and J. H. Weber (TUMQCD), Phys. Rev. D **107**, 074503 (2023), arXiv:2206.03156 [hep-lat].
- [35] M. Cheng *et al.*, Phys. Rev. D **77**, 014511 (2008), arXiv:0710.0354 [hep-lat].
- [36] A. Bazavov, N. Brambilla, H. T. Ding, P. Petreczky, H. P. Schadler, A. Vairo, and J. H. Weber, Phys. Rev. D **93**, 114502 (2016), arXiv:1603.06637 [hep-lat].
- [37] M. Luscher, Nucl. Phys. B **180**, 317 (1981).
- [38] M. Luscher and P. Weisz, JHEP **07**, 049 (2002), arXiv:hep-lat/0207003.
- [39] M. Luscher, K. Symanzik, and P. Weisz, Nucl. Phys. B **173**, 365 (1980).
- [40] O. Alvarez, Phys. Rev. D **24**, 440 (1981).
- [41] M. Laine and Y. Schroder, JHEP **03**, 067 (2005), arXiv:hep-ph/0503061.
- [42] M. J. Teper, Phys. Rev. D **59**, 014512 (1999), arXiv:hep-lat/9804008.
- [43] D. Karabali, C.-j. Kim, and V. P. Nair, Phys. Lett. B **434**, 103 (1998), arXiv:hep-th/9804132.
- [44] C. E. Detar and J. B. Kogut, Phys. Rev. Lett. **59**, 399 (1987).
- [45] A. Bazavov *et al.*, Phys. Rev. D **100**, 094510 (2019), arXiv:1908.09552 [hep-lat].
- [46] B. B. Brandt, A. Francis, H. B. Meyer, O. Philipsen, D. Robaina, and H. Wittig, JHEP **12**, 158 (2016), arXiv:1608.06882 [hep-lat].
- [47] M. Cheng *et al.*, Eur. Phys. J. C **71**, 1564 (2011), arXiv:1010.1216 [hep-lat].
- [48] M. Dalla Brida, L. Giusti, T. Harris, D. Laudicina, and M. Pepe, JHEP **04**, 034 (2022), arXiv:2112.05427 [hep-lat].
- [49] E. Eichten and F. Feinberg, Phys. Rev. D **23**, 2724 (1981).
- [50] V. Koch, E. V. Shuryak, G. E. Brown, and A. D. Jackson, Phys. Rev. D **46**, 3169 (1992), [Erratum: Phys.Rev.D 47, 2157 (1993)], arXiv:hep-ph/9204236.
- [51] L. Giusti, M. L. Paciello, C. Parrinello, S. Petrarca, and B. Taglienti, Int. J. Mod. Phys. A **16**, 3487 (2001), arXiv:hep-lat/0104012.
- [52] L. Giusti, T. Harris, D. Laudicina, M. Pepe, and P. Rescigno, Phys. Lett. B **855**, 138799 (2024), arXiv:2405.04182 [hep-lat].
- [53] L. Mazur *et al.* (HotQCD), Comput. Phys. Commun. **300**, 109164 (2024), arXiv:2306.01098 [hep-lat].
- [54] A. Bazavov, H. T. Ding, P. Hegde, F. Karsch, C. Miao, S. Mukherjee, P. Petreczky, C. Schmidt, and A. Velytsky, Phys. Rev. D **88**, 094021 (2013), arXiv:1309.2317 [hep-lat].
- [55] E. Follana, Q. Mason, C. Davies, K. Hornbostel, G. P. Lepage, J. Shigemitsu, H. Trottier, and K. Wong, Phys. Rev. D **75**, 054502 (2007).

- [56] G. P. Lepage, Phys. Rev. D **59**, 074502 (1999).
- [57] A. Bazavov, C. Bernard, C. DeTar, W. Freeman, S. Gottlieb, U. M. Heller, J. E. Hetrick, J. Laiho, L. Levkova, M. Oktay, J. Osborn, R. L. Sugar, D. Toussaint, and R. S. Van de Water (MILC Collaboration), Phys. Rev. D **82**, 074501 (2010).
- [58] O. Philipsen, Nucl. Phys. B **628**, 167 (2002), arXiv:hep-lat/0112047.
- [59] O. Philipsen, Phys. Lett. B **535**, 138 (2002), arXiv:hep-lat/0203018.
- [60] A. Bazavov, T. Bhattacharya, C. DeTar, H.-T. Ding, S. Gottlieb, R. Gupta, P. Hegde, U. M. Heller, F. Karsch, E. Laermann, L. Levkova, S. Mukherjee, P. Petreczky, C. Schmidt, C. Schroeder, R. A. Soltz, W. Soeldner, R. Sugar, M. Wagner, and P. Vranas (HotQCD Collaboration), Phys. Rev. D **90**, 094503 (2014).
- [61] A. Bazavov, T. Bhattacharya, M. Cheng, C. DeTar, H.-T. Ding, S. Gottlieb, R. Gupta, P. Hegde, U. M. Heller, F. Karsch, E. Laermann, L. Levkova, S. Mukherjee, P. Petreczky, C. Schmidt, R. A. Soltz, W. Soeldner, R. Sugar, D. Toussaint, W. Unger, and P. Vranas (HotQCD Collaboration), Phys. Rev. D **85**, 054503 (2012).
- [62] P. Giovannangeli, Phys. Lett. B **585**, 144 (2004), arXiv:hep-ph/0312307.
- [63] Y. Aoki *et al.* (Flavour Lattice Averaging Group (FLAG)), Eur. Phys. J. C **82**, 869 (2022), arXiv:2111.09849 [hep-lat].
- [64] B. Schmidt and M. Steinhauser, Comput. Phys. Commun. **183**, 1845 (2012), arXiv:1201.6149 [hep-ph].
- [65] Y. Schroder, *The Static potential in QCD*, Ph.D. thesis, Hamburg U. (1999).